Earthquakes and Structures, *Vol. 8, No. 1 (2015) 19-35*
DOI: http://dx.doi.org/10.12989/eas.2015.8.1.019

Seismic performance of gravity-load designed concrete frames infilled with low-strength masonry

Umair A. Siddiqui[a], Haluk Sucuoğlu[*] and Ahmet Yakut[b]

Department of Civil Engineering, Middle East Technical University, Ankara - Turkey

(Received November 5, 2013, Revised July 1, 2014, Accepted July 7, 2014)

Abstract. This study compares the seismic performances of two reinforced concrete frame specimens tested by the pseudo-dynamic procedure. The pair of 3-storey, 3-bay frames specimens are constructed with typical characteristics of older construction which is lacking seismic design. One of the specimens is a bare frame while the other is infilled with low-strength autoclave aerated concrete (AAC) block masonry. The focus of this study is to investigate the influence of low strength masonry infill walls on the seismic response of older RC frames designed for gravity loads. It is found that the presence of weak infill walls considerably reduce deformations and damage in the upper stories while their influence at the critical ground story is not all that positive. Infill walls tend to localize damage at the critical story due to a peculiar frame-infill interaction, and impose larger internal force and deformation demands on the columns and beams bounding the infills. Therefore the general belief in earthquake engineering that infills develop a second line of defence against lateral forces in seismically deficient frames is nullified in case of low-strength infill walls in the presented experimental research.

Keywords: gravity-load design; infilled frames; low-strength infills; AAC; pseudo-dynamic testing; performance evaluation

1. Introduction

There is a large stock of existing reinforced concrete buildings in seismic regions around the world which are not designed and/or constructed according to the regulations of present seismic codes and best practices. Devastating earthquakes in seismically active regions of the World during the last decades have revealed growing concerns about the performance of these deficient buildings. Their frames are mostly infilled with masonry walls which affect their seismic performance usually in a complicated way due to the interaction of masonry infill panels with the primary structural elements in resisting seismic actions. An enormous quantity of experimental and analytical research has been conducted in the past to study the effects of clay and concrete masonry infills on the seismic response of new and existing reinforced concrete frames (Polyakov, 1960; Stafford-Smith, 1966, 1967, 1969; Klingner and Bertero 1978; Pujol and Fich 1979; Bertero

*Corresponding author, Professor, E-mail: sucuoglu@metu.edu.tr
[a]Ph.D. Student, E-mail: e189324@metu.edu.tr
[b]Professor, E-mail: ayakut@metu.edu.tr

http://www.techno-press.org/?journal=eas&subpage=7 ISSN: 2092-7614 (Print), 2092-7622 (Online)

and Brokken 1983; Mehrabi *et al*. 1996; Fardis and Panagiotakos 1997; Mosalam *et al*. 1998; Buonapane and White 1999; Crisafulli *et al*. 2000; Al-Chaar *et al*. 2002; Lee and Woo 2002; Magenes and Pampanin 2004; Fiore *et al*. 2012; Uva *et al*. 2012). Despite this wealth of information, direct contribution of masonry infills to seismic response of buildings are usually disregarded in the design of new buildings as well as the evaluation of existing buildings other than their weight and mass.

Eurocode 8-1 (2004) imposes additional measures in the design of masonry infilled concrete frames which are classified as high ductility. The entire length of those columns adjacent to a masonry infill wall from one side are considered as critical region, and detailed accordingly. Moreover, shear forces transmitted to the boundary columns due to the diagonal strut action of the masonry panel are calculated quite conservatively, and imposed on the column as additional design shear force along the contact length. It is required to consider the possible irregularities in plan and elevation developed by the uneven distribution of infill walls, and their adverse effects on seismic actions. Light wire meshes anchored on a wall face, or wall anchorages to the boundary columns are advised in order to prevent disintegration of the wall panels from the frame. ASCE 41 (2006) considers masonry infills as structural members in seismic assessment of infilled frames where the infill acts as an equivalent compression strut in a diagonally braced concrete frame and the bounding columns are considered as tension-compression chords.

Majority of the research on the seismic response of infilled frames had been conducted with strong unreinforced masonry infill walls. However the use of light-weight block masonry walls are gaining familiarity in the construction of partition walls due to their low weight as well as easier workability. Autoclaved Aerated Concrete (AAC) is a typical example of light weight masonry, with excellent fire resistance and thermal insulation capabilities which are ideal for seismic design and risk reduction. Further, light infill panels have much lower risk for out of plane failure during seismic excitation. Hence, there is a need for research in order to study the seismic response of RC frames constructed with low-strength masonry infill walls.

The first task of this study is to provide experimental data on the seismic performance of gravity load designed reinforced concrete frames subjected to actual ground motions. Two ½ scale 3-story, 3-bay seismically deficient concrete frames were tested by using the pseudo-dynamic testing procedure under three consecutive ground motions with progressively increasing intensity levels. Then the seismic performances of the bare and infilled frames are evaluated comparatively in terms of both the global and local responses, which is the second task of the presented study.

2. Test specimens

The typical test frame comprises of the interior bay frame (Grid-3) of the prototype three-story building (Fig. 1a). The dimension of columns with 1.33% of longitudinal reinforcement ratio was 400 × 300 mm while the beam dimensions were 300x350 mm. Test frames were ½ scaled specimens of the prototype shown in Figs. 1(b) and 1(c).

The 3-storey, 3-bay frame specimens are constructed with material and detailing characteristics of old, gravity designed frames commonly observed around the world. The first specimen is a bare frame, hereinafter referred as Specimen #1, while the second frame, hereinafter referred as Specimen #2 is infilled with AAC block masonry in the middle bay. The average concrete

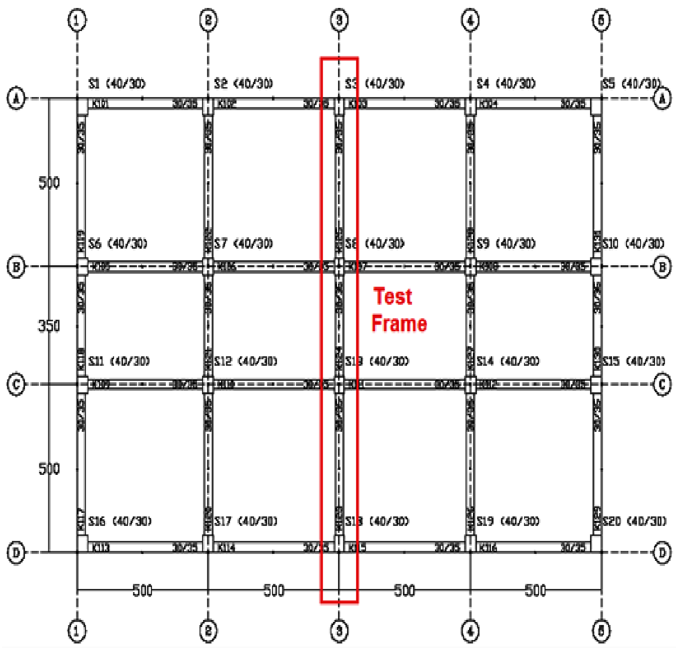

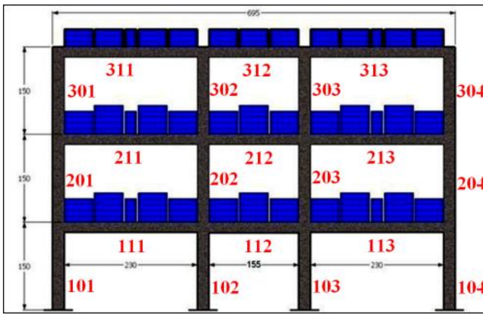

b) Elevation view of specimen #1

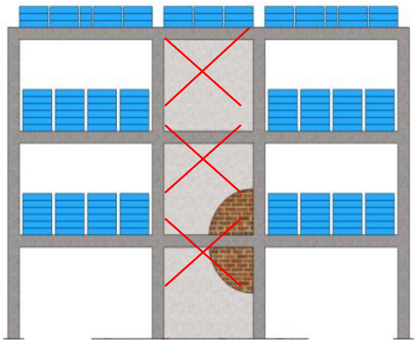

a) Plan view of prototype building and test frame c) Elevation view of specimen #2

Fig. 1 Plan view of the prototype building (a), and the elevations of the two test frames (b and c) with element labels (Dimensions are in cm)

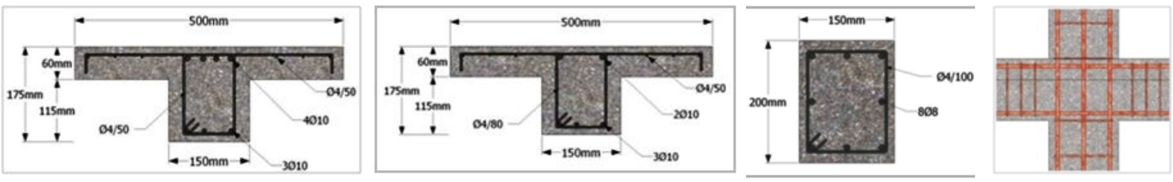

Beam (Support Regions) Beam (Span Regions) Column (Typical) Typical Joint

Fig. 2 Column and beam reinforcement details for Specimen #1 and #2

Table 1 Moment and shear capacities of columns and moment capacities of beams

Specimen	Loc.	Column				Beams			
		Moment Capacity [kN-m]		Shear Capacity [kN]	Shear Demand [kN]	Moment Capacity [kN-m]			
		Yield	Plastic			Yield		Plastic	
						Span	Support	Span	Support
		M_y	M_p	V_r	V_e	M_y	M_y	M_p	M_p
# 1 [Bare Frame]	Outer Inner	13.0 13.4	14.1 14.8	26.6	18.4	17.8	12.7	20.7	16.8
# 2 [Infilled Frame]	Outer	13.2	14.8	28.4	18.6	18.0	12.9	21.0	17.0

compressive strength for these specimens were 12.9 MPa for Specimen #1 (SP #1) and 14.1 MPa for Specimen #2 (SP #2). The yield strength of plain reinforcing bars, determined from material tests, for columns and beams of both specimens were 320 and 355 MPa respectively whereas the yield strength of transverse reinforcing bars for both specimens was 240 MPa. The spacing of transverse reinforcement of the columns was kept constant throughout the column height, which resulted in unconfined end-zones at potential plastic hinge regions of the element. Lateral reinforcement from the column members did not continue into the joints, reflecting joint shear deficiencies.

Gravity loads calculated from the 3D prototype building are applied to the 2D specimens using the steel blocks shown in Fig. 1. Gravity loads are taken as 4 kN/m2 corresponding to the line load of 15.7 kN/m. The axial load ratios of the first story exterior and interior columns under gravity loads are 15.5% and 25.8% for SP #1, and 15.44% and 19.0% for SP #2, respectively.

AAC infill walls in SP #2 had the thickness of 150 mm, same as the enclosing frame members. The compressive strength of AAC was 2.6 MPa, which was determined from the compressive prism tests. The catalogue value for the compressive strength of AAC blocks is 2.5 MPa. Infill panels and the blocks have almost the same compressive strength because the blocks are connected with a very thin and strong glue in constructing the panels. Hence the joints between the blocks practically do not affect the compressive strength of infill panels.

The flexural and shear capacity of the beams and columns were designed to be sufficient only for gravity loads. The detailing of reinforcement in beams and columns is such that the system has strong beam-weak column condition, contrary to the general code provisions. Typical detailed drawings of specimens are shown in Fig. 2. Table 1 indicates the moment and shear capacities of columns and beams. Column shear demand under gravity loads only is also shown. The shear capacities of columns are larger than the associated shear force demand, hence assuring flexural response.

3. Pseudo dynamic testing

Pseudo-dynamic testing (also referred to as the online computer controlled testing) is a hybrid earthquake simulation technique which enables to model part of the dynamic structural properties numerically while rest of the structure is physically tested in parallel with computations, as often demonstrated (Mahin and Shing, 1985). This testing method has been developed as a convenient and realistic alternative to the more advanced shake table testing and introduced greater accuracy providing the simplicity of conventional methods like quasi-static testing. Other attributes are the ability to observe general response and resulting damage formation in structure during the test because the seismic loading is applied in prolonged time or “pseudo-time” rather than in real time. Pseudo dynamic testing is limited to structures with lumped masses where the inertial forces develop along the dynamic degrees of freedom. This limitation is not critical to the test structure since all story masses are lumped along the lateral displacement degrees of freedom of each story.

The main difference between pseudo-dynamic test and true dynamic testing is that at each pseudo time step, the computed structural displacements are actually applied to the structure and the resulting restoring forces are measured experimentally by the load cells. This removes the uncertainty linked with the analytical modelling of restoring forces of the structure. The time step employed in the PsD control algorithm is 0.003535 seconds. A short time step is crucial for capturing sudden stiffness changes due to

a) Pseudo-dynamic testing scheme b) Elevation of bare frame c) Elevation of infilled frame

Fig. 3 Pseudo-dynamic testing scheme (a) and test specimens (b and c)

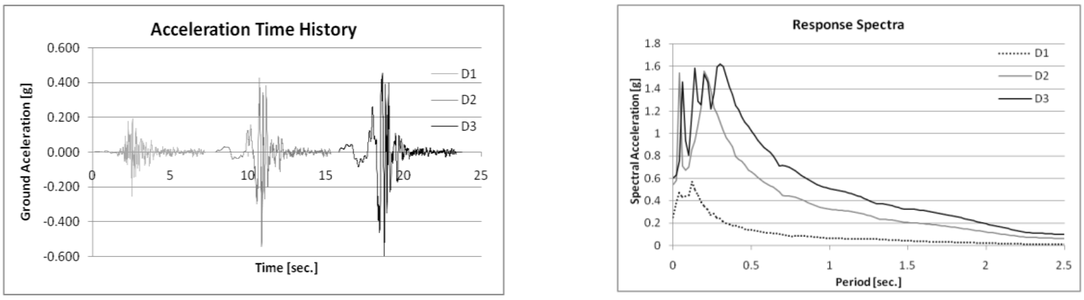

Fig. 4 Acceleration time-series (a) and response spectra (b)

Table 2 Ground Motion Properties

Earthquake GM	Probability of Exceedance in 50 Years	Soil Class/Type	PGA [g]
D1	50%	Rock	0.254
D2	10%	Rock	0.545
D3	10%	Soft soil	0.604

cracking or yielding of members, or sudden stiffness recovery due to crack closing during testing. LVDTs were used to measure story displacements, curvatures and rotations at the bottom of the base columns andthe extreme ends of all beams at the 1st and 2nd storeys as well as strains in the infill panels on all three storeys.

Pseudo dynamic testing scheme is shown graphically in Fig. 3(a). Elevations of bare and infilled frames are shown in Figs. 3(b) and 3(c). Each test specimen has three translational degrees of freedom.

Ground motions used for these pseudo-dynamic tests are presented in Fig. 4, which consists of synthetic time-acceleration series of the 1999 Düzce earthquake. They are compatible with the site-specific earthquake design spectra for different exceedance probabilities on different soil types, as shown in Table 2 and plotted in Fig. 4. Three generated acceleration series (named D1, D2, and D3) imposed on the test specimens sequentially are presented in Fig. 4 along with their corresponding acceleration spectra.

4. Test results

This section presents the pseudo-dynamic test results of both specimens. Time variation of roof displacements, first story drift ratios and first story shear forces are presented respectively in Figs.

5, 6 and 7 for both specimens.

The roof displacement time history of both specimens in Fig. 5 indicates that presence of infills in SP #2 results in reducing the peak roof displacement considerably, up to about 55 percent during strong shaking in D3 as compared to bare frame. Significant reduction of up to 70 percent is also seen in the residual roof displacement of AAC infilled frame. The situation is quite different however for the first story inter-story drift comparison presented in Fig. 6. This figure indicates that until the first cracking of infill (point A in Fig. 5 during D2), interstory drift ratios of both specimens were similar. However immediately after cracking of infill shown by an arrow in Fig. 6, interstory drift abruptly increased during the reverse cyclic motion compared to that of bare frame, by up to 18 percent. Similar response is observed in the second story as well.

Sudden cracking of brittle AAC panels was the cause of sudden drift increase at the first story which followed the sudden drop in the stiffness of the infilled frame. Such an instantaneous response of the PsD control algorithm to sudden stiffness change is also an indication of its effectiveness.

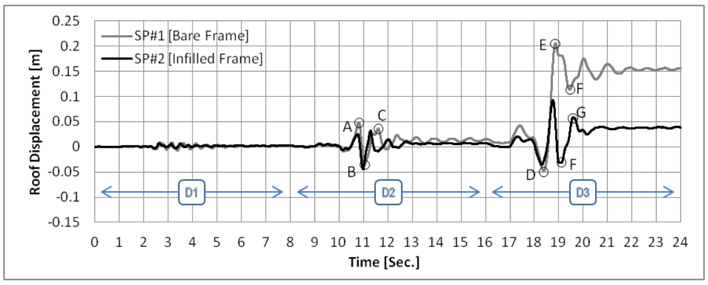

Fig. 5 Roof displacement time-history (SP#1 and SP#2)

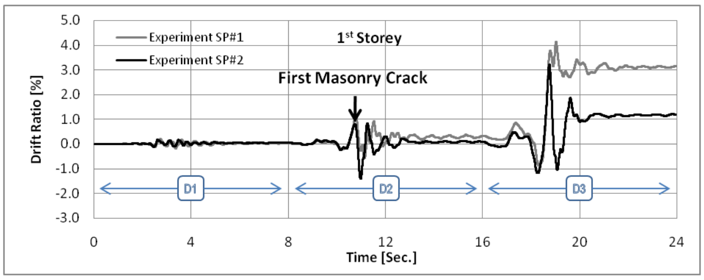

Fig. 6 First story drift ratio time-history (SP#1 and SP#2)

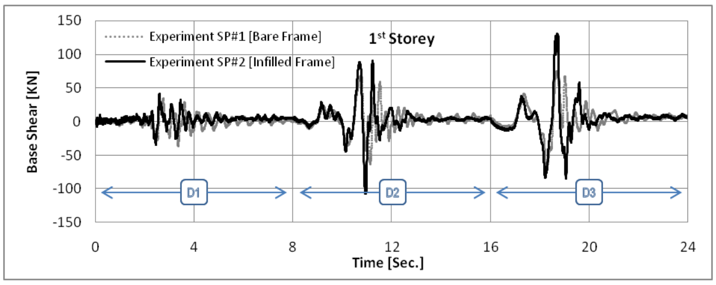

Fig. 7 First story (base) shear force time-history (SP#1 and SP#2)

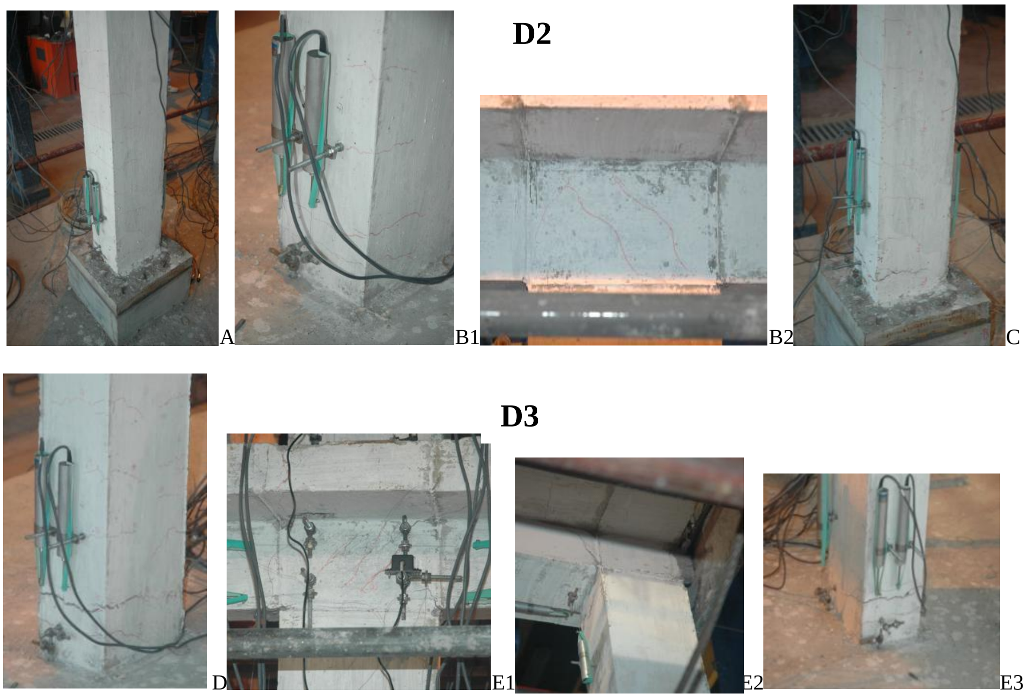

A Flexural cracks at 1st storey exterior column (D2)
B1 Flexural cracks at 1st storey interior column (D2)
B2 Diagonal cracks at 1st storey interior joint (D2)
C Flexural cracks at 1st storey exterior column (D2)
D Flexural cracks at 1st storey interior column (D3)
E1 Diagonal cracks at 1st storey interior joint (D3)
E2 Shear crack at 1st storey exterior beams ends
E3 Flexural cracks at 1st storey interior columns (D3)

Fig. 8 Damage evolution at the exterior and interior columns, interior joint and beam connecting to the exterior joint of the first story, during D2 (upper row) and D3 (lower row) of SP#1.

The base shear time histories presented in Fig. 7 reveals that base shear is considerably greater in infilled frame at the instants of peak drifts during D1, D2 and D3, by about 14%, 56% and 73 % respectively. This indicates that despite the weak AAC infill masonry which is filling only the shorter bay of the three bays, infill panel takes over and attract greater shears once the deficient frame suffers damage.

4.1 Damage evolution in the bare frame

Step-by-step gradual damage evolutions of each specimen during the tests are presented in Figs. 8 and 9 respectively for SP#1 and SP#2. Damage evolution in both specimens are referred to the roof displacement peak sequences shown in Fig. 5.

Damage states of the bare frame SP#1 are shown Fig. 8. It exhibits no damage during D1, and moderate damage during D2. Flexural cracks occur at the bases of both exterior and interior and columns in the form of single dominant flexural crack due to bond slip, typical of plain longitudinal reinforcement. During severe ground motion D3, both columns fail in flexure at their bases with the opening of the same single dominant crack. Weak column-strong beam condition prevails at the interior joints. Hence no damage occurred at the beam ends during D2. However interior joints cracked during D2 which further intensified during D3, indicating significant joint panel deformation. Finally, the beam end connecting to the exterior joint failed in shear-flexure during D3.

4.2 Damage evolution in the Infilled frame

During the first ground motion D1, no apparent damage was noted in any of the structural members of the specimen. In addition none of the masonry panels suffered visible damage except minor separation cracks along the boundary of the panel and boundary frame at first storey. The specimen was at the minor damage state at the end of ground motion D1.

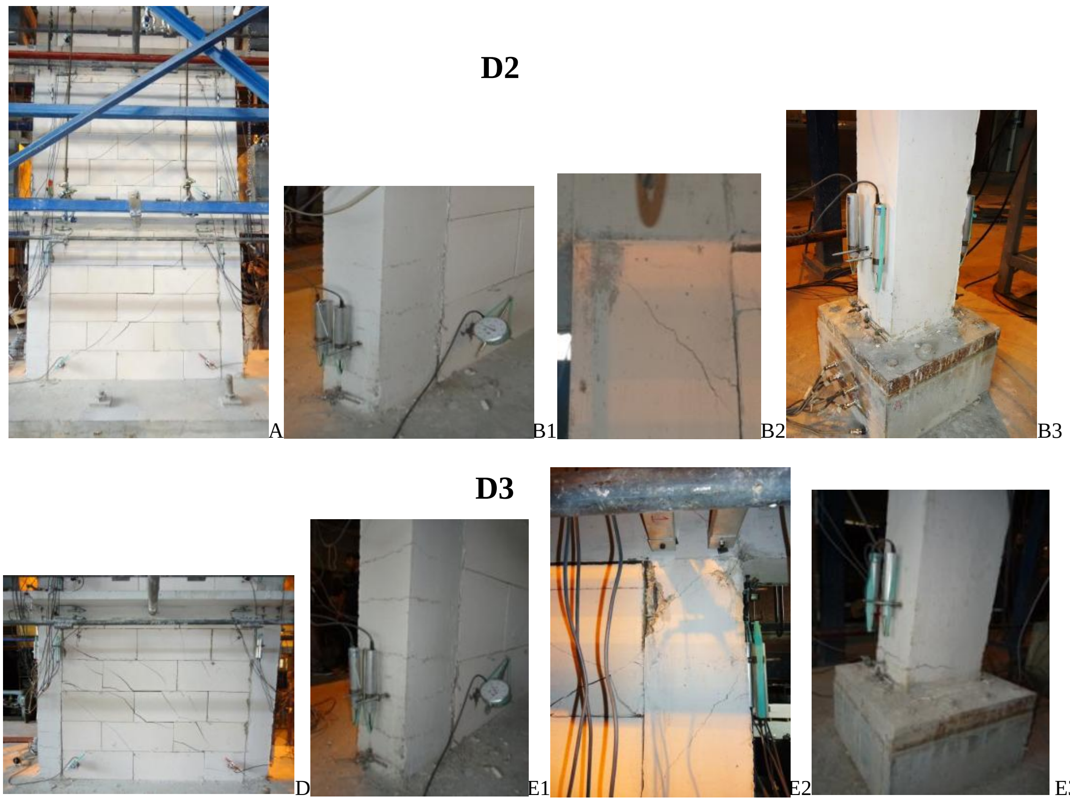

A	Diagonal crack at 1st and 2nd storey infill Panels (D2)	**B1**	Flexure cracks at 1st storey bounding column bottom (D2)
B2	Diagonal crack at 1st storey bounding column top (D2)	**B3**	Minor flexure cracks at 1st storey exterior column bottom (D2)
D	Diagonal cracks at 1st storey infill Panels (D3)	**E1**	Flexure cracks at 1st storey bounding column bottom (D3)
E2	Diagonal cracks at 1st storey bounding column top (D3)	**E3**	Flexure cracks at 1st storey exterior column bottom (D3)

Fig. 9 Damage evolution at the infill, interior columns and exterior columns of the first story, during D2 (upper row) and D3 (lower row) of SP#2

Infill panels of frame SP#2 shown Fig. 9 displayed diagonal tensile cracking during D2. These cracks have widened and the family of diagonal cracks increased during D3. Interior columns bounding the infill panels exhibited distributed cracking along their length, indicating that they respond as tension-compression chord which is indeed foreseen by ASCE 41. However the compressive force which developed at the diagonal strut exerted additional shear to the top of bounding columns, which eventually caused shear cracking during D2, and shear failure during D3. Although the compressive strength of AAC is low, apparently it is sufficient to cause shear failure of the deficient boundary columns.

Shear failure in boundary columns indicates the exceedance of their shear capacity of 28.4 kN given in Table 1. At this onset of column shear cracking and panel cracking, the maximum base shear of infilled and bare frames are 107 kN and 44 kN respectively. If the difference of these, i.e. 107 - 44 = 63 kN is assumed to be resisted by the panel until it cracked, then this amount of shear transfer to the column is more than enough to exceed its shear capacity. In fact, if only half the shear from the panel goes to the column, assuming the other half is redistributed to the beam, it is still greater than the shear capacity of the column.

In terms of peak drift during the strong shaking D3, the infills however contribute significantly in limiting the peak inter-story drift ratio to 3.22 percent as compared to 4.13 percent of the bare frame. The residual drift of infilled frame is also considerably reduced up to about 70 percent. The cracking drift Δ_{cr} i.e. the drift at which first crack appears in the AAC infill was recorded as 0.53 percent which is more or less the same for higher story panels. At the drift of about 1.45 percent, the infills at the 1st and 2nd stories suffered severe damage and the integral behaviour of infill and masonry was no longer present.

The exterior columns have benefitted from the AAC infills since the crack widths were less in SP#2 compared to SP#1, both during D2 and D3.

4.3 Failure modes of the bare and the infilled frame

From the observations above, it is apparent that both of the specimens suffered severe damage at the end of ground motion D3. These damages resulted in large plastic deformations in both specimens. However, the dominant cause of plastic deformations for both specimens differs greatly from each other.

The bare frame failed in flexure at the bottom ends of the first storey column and at top ends of the second storey columns, but the failure was abrupt. Although some ductility was present, the ample warning usually associated with the flexural failure was absent. This was somehow expected because the frame elements were not designed for seismic loading and were not detailed for ductility.

The failure of the infilled frame was also governed by the failure of first story columns, however the failure modes of columns differ from each other. The exterior columns depicted flexure failure at the bottom ends, but the failure was not ductile similar to the one observed in the bare frame. On the other hand, the failure of interior columns surrounding the infill panel was brittle, caused by excessive diagonal shear cracking at the column tops. The cracking thereby resulted in spalling of concrete and buckling of reinforcement. The main cause of such failure is the transfer of additional shear stresses from the loaded diagonal of the infill panel to the column top and the absence of adequate shear reinforcement to resist these stresses.

5. Comparative evaluation of test results for bare and infilled frames

This section evaluates the experimental performances of both frames comparatively, in terms of global and local response parameters.

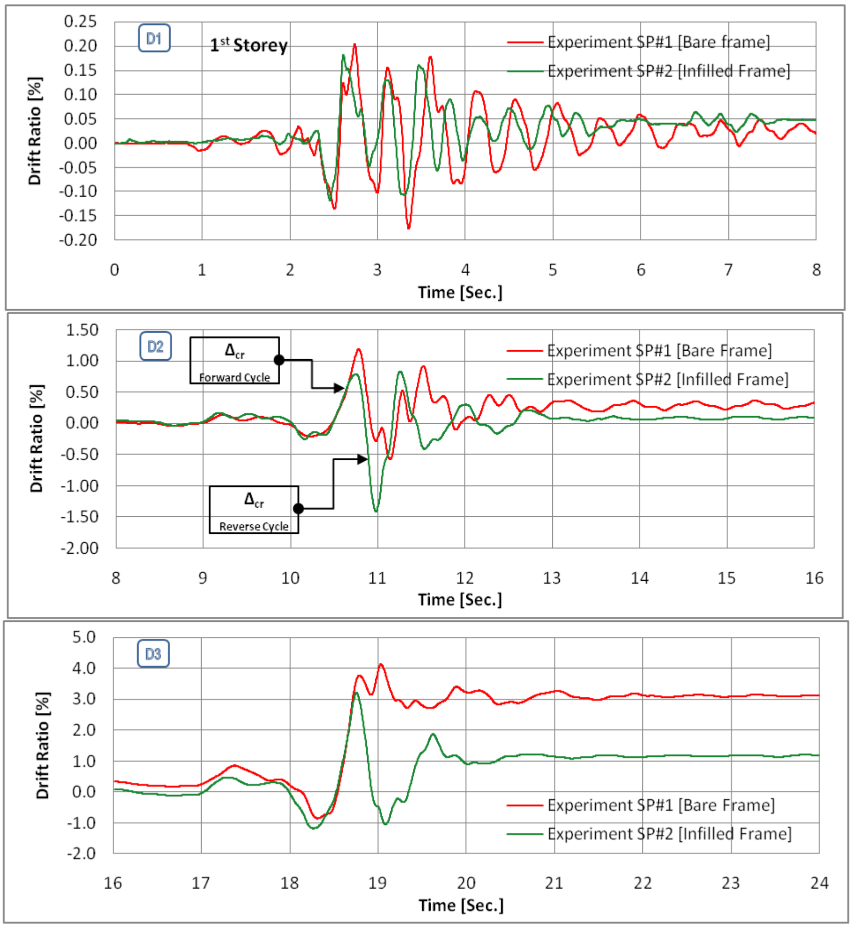

Fig. 10 First story drift time histories

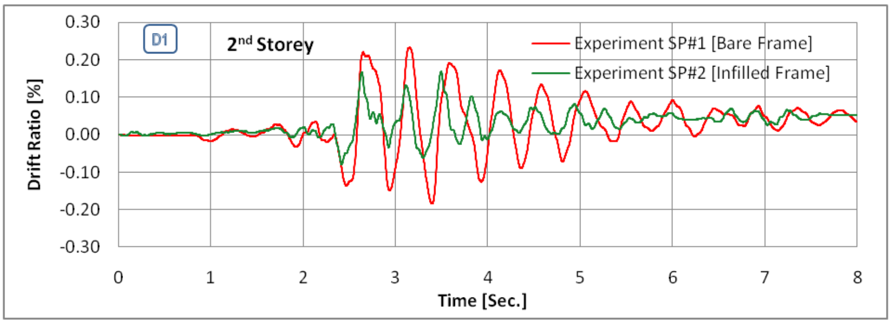

Fig. 11 Second story drift time histories

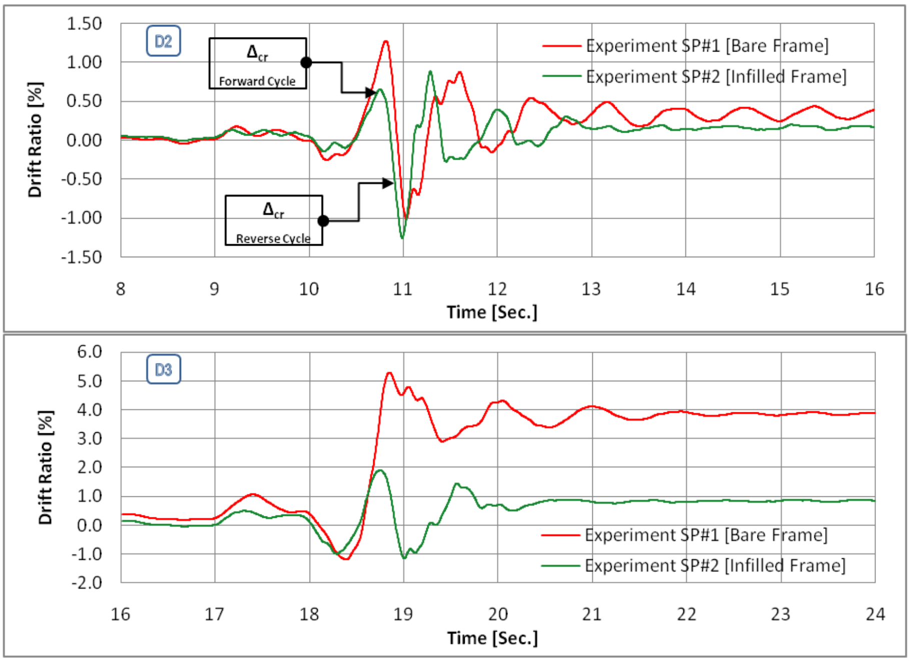

Fig. 11 Continued

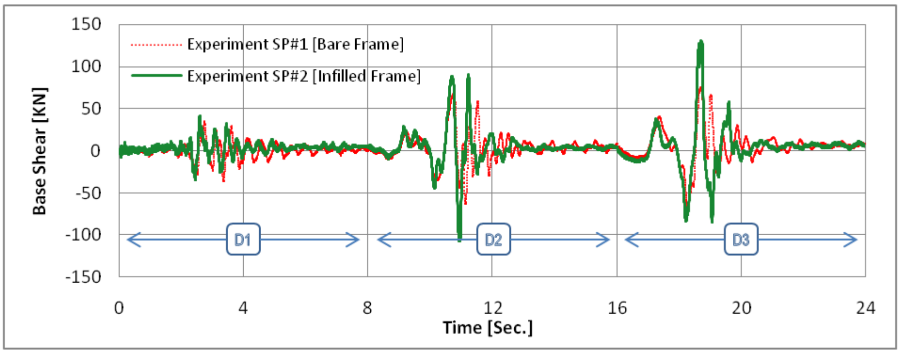

Fig. 12 First story shear (base shear) time history

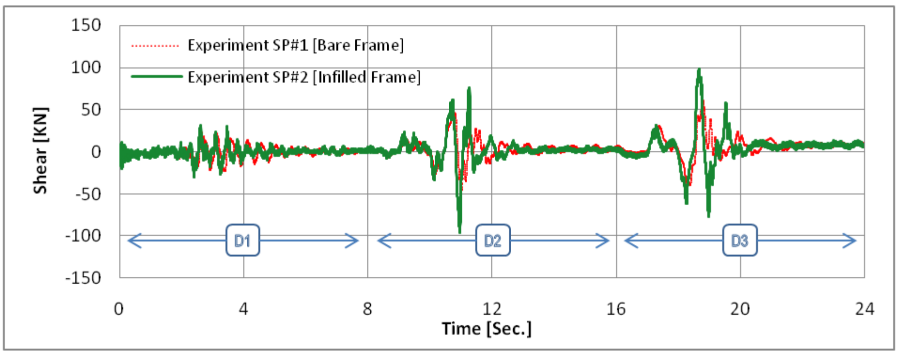

Fig. 13 Second story shear time history

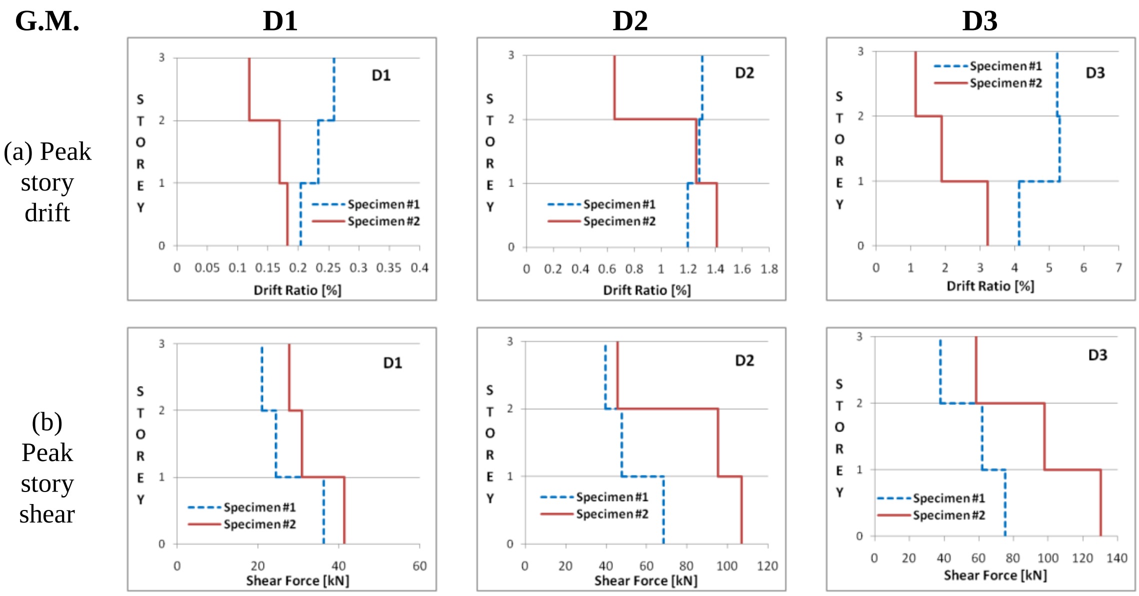

Fig. 14 Comparison of peak inter-story drifts (a) and peak story-shears (b) between SP#1 and SP#2

5.1 Comparison of global responses

Global response comparisons include force and deformation responses and energy dissipation under low, moderate and high intensity ground motions. Interstory drift and shear time histories of both specimens at the first two stories are shown in Figs. 10-11 and 12-13, respectively. Distributions of peak interstory drifts and peak storey shears for the bare and infilled frames under each ground motion are presented in Fig. 14. Story hysteresis diagrams are plotted in Fig. 15 for both specimens. Hysteretic energy variations with time at all three stories are given in Fig. 16. All data presented in these figures are derived from the measured story displacement and story shear force time histories. Hence they are all related, but expressed in terms of different response parameters. The following observations can be derived from the comparative evaluation of the presented global response data.

1. Infill walls are effective in reducing the drifts at the upper stories (Figs. 11 and 14(a)).
2. Infill walls are effective in reducing the residual drifts at all stories (Figs. 10, 11 and 15).
3. Following the cracking of infill at the first story during D2, larger peak interstory drift occurs in the first story of infilled frame compared to the bare frame (Fig. 10). The probable cause of such drift increase in the infilled frame is the occurrence of shear failure in the first story bounding columns at the same instant (Point B2 in Fig. 9).
4. As the damage in the gravity load designed frame increases with ground motion intensity from D1 to D2 and further to D3, infill panels at all stories attract greater share of story shears (Figs. 12 and 13).
5. Peak interstory drift at the critical first story level is not affected significantly by the presence of infills under all three ground motions. However the influence of infills in reducing story drifts is more significant at the less critical upper stories. Infill wall at the base receives

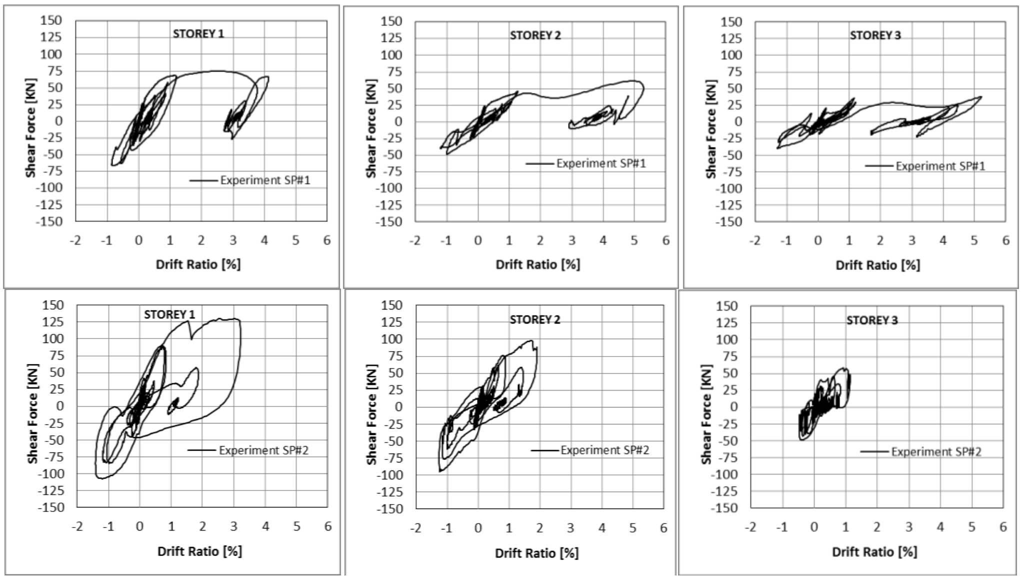

Fig. 15 Story hysteresis diagrams (story shear versus interstory drift ratio) for the test specimens SP#1 (bare) and SP#2 (infilled)

larger share of the base shear force as the damage in the RC members increase with the increase in the intensity of earthquake (Fig. 14(b)), however this does not lead to reducing interstory drift at the first story (Fig.14(a)).

6. Weak infills alter the deformation behavior and place major deformation demand on the first story (Fig. 14(a)). This is critical, since a complete failure of the first story infill may likely result in a soft story collapse mechanism.

7. Presence of weak infills in the gravity load designed frame is apparently developing a more stable hysteretic response in all three stories, however localization of damage at the critical story is manifested by the large deformation cycle during D3 (Fig. 15).

8. Infills increase hysteretic energy dissipation significantly. However this increase comes mostly from the ground story, and there is no increase at the third story (Fig. 16), indicating damage localization at the first story.

5.2 Comparison of local responses

The time variations of the bottom end rotations of columns 101 and 102 and the end rotations of beam 111 are presented comparatively for both test specimens in Figs. 17 and 18. End rotations of the columns 101 (exterior) and 102 (interior) of the 1st story in Fig.17 indicate that infilled frame has similar response as of the bare frame during D1 because of the absence of frame-infill composite action. During D2, the maximum end rotations at the bottom ends of both columns are lower in the infilled frame than the bare frame. At the end of ground motion D2, due to the flexural cracking in column bottom ends, some residual rotations appear in the bare frame columns which are well contained by the infills in the case of infilled frame. During ground motion D3, the peak rotations for both frames are essentially similar because of the formation of

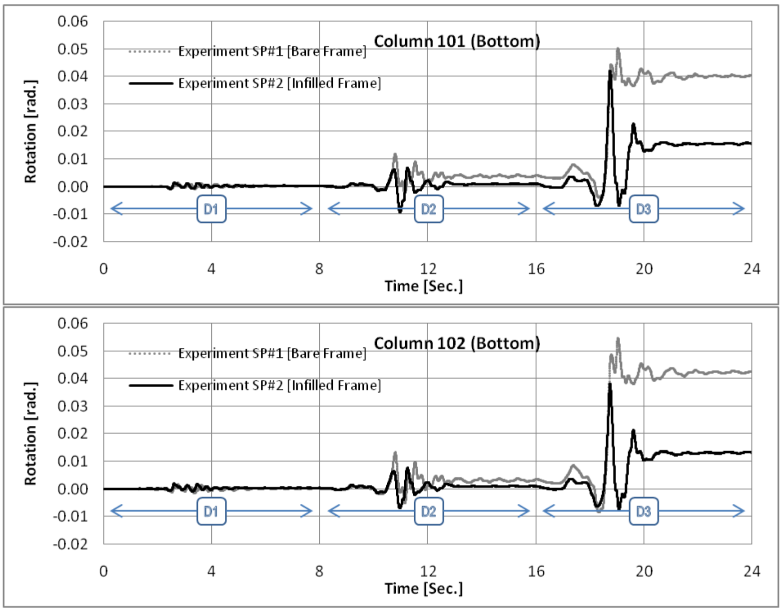

Fig. 17 End rotation time-history for columns 101 and 102 (SP#1 and SP#2)

flexural plastic hinges and large plastic rotations which imply severe damage. However infills notably reduce the residual rotations as also evident from the global responses.

The end rotations of the exterior beam (111) of the 1st storey are shown in Fig. 18. It is to note that in the infilled specimen, beam-111 is not bounding the infill panel but rather it is connecting to beam 112 which bounds the infill panel at the 1st storey. The rotation response at both ends indicates a significant increase in peak rotations of beam-111 in the infilled frame as compared to the bare frame during both D2 and D3 ground motions.

During the D2 ground motion, the bottom end rotations of the first story columns in the bare frame exceed 1% while all other column and beam end rotations remain below 1%. The presence of infills alters this distribution in the infilled frame, however the level of end rotations does not differ notably. It has been observed that the general deformation performances of the bare and the infilled frames are quite similar under the moderate intensity D2 ground motion, hence the contribution of low strength infills to frame performance is not significant. This conclusion is consistent with the maximum interstory drift distributions presented in Fig. 14(a).

Rotations at the first story column bottom ends of the bare frame exceed 5% under the severe D3 ground motion, indicating a collapse performance. These rotations reduce to 4% on average in the infilled frame, but still indicating collapse performance. Although the end deformations of columns and beams in the upper stories reduce considerably in the infilled frame, damage localizes at the first story. This is also consistent with the maximum interstory drift distribution presented in Fig. 14(a) under D3. Moreover, additional shear forces imposed by the diagonal strut in the first story leads to shear failure in the boundary column (Fig. 9-E2) and the infill itself is severely damaged (Fig. 9-A). Accordingly, presence of infills does not upgrade the seismic performance of concrete frame under the higher intensity ground motion.

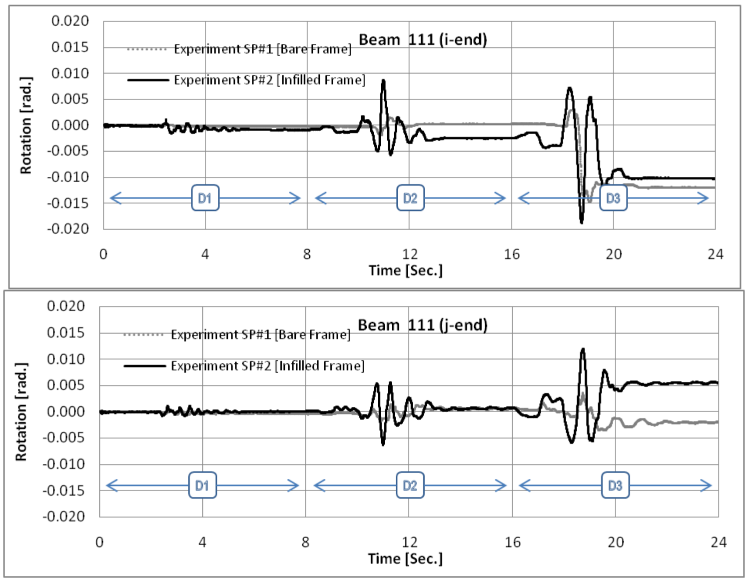

Fig. 18 End rotation time-history for beam 111 (SP#1 and SP#2)

6. Conclusions

Seismic response of gravity-load designed bare and infilled concrete frames are investigated in this study by conducting pseudo dynamic testing on a pair of 3-storey, 3-bay RC frames. Low strength AAC panels were employed as the infills. Comparisons are provided between the bare frame and the corresponding infilled frame responses by using experimental test results in terms of primary failure modes, global response parameters and local response parameters. The following conclusions can be drawn from the comparative evaluation of test results.

1. Low strength infills do not improve the seismic response of gravity-load designed concrete frames under moderate intensity ground motions.
2. The contribution of infills to seismic response is more significant under higher intensity ground motions. They reduce deformations in the upper stories considerably, however their effect on the mostly stresses first story is limited. Damage is localized more at the ground story compared to the bare frame which is a disadvantage from the seismic stability perspective.
3. Infills reduce residual drifts of the frame significantly, which is the most notable positive contribution of low strength infills to the seismic performance of gravity load designed frame.
4. In seismically deficient construction, infill panels attract significant amount of shear force but cause localized shear failure in the bounding columns at the potential diagonal strut regions, especially at the lowest story. Moreover, severe damage displayed by the infills at the lower stories further reduces the infilled frame performance.
5. Experimental observations revealed that the presence of low strength infill walls in gravity-load designed concrete frames do not reduce the overall damage in the infilled frame under both moderate and high intensity ground motions. This is against the general belief in earthquake engineering that infills develop a second line of defence against lateral forces in seismically deficient frames.

Acknowledgement

This study was conducted with the financial support provided by the Turkish Scientific and Technological Research Council (TUBITAK) with the Grant No: 108G034.

References

Al-Chaar, G., Issa, M. and Sweeney, S. (2002), “Behaviour of masonry- infilled non-ductile reinforced concrete frames”, *J. Struct. Eng. (ASCE)*, **128**(8), 1055-1063.

American Society of Civil Engineers (2006), “Seismic rehabilitation of existing buildings”, *ASCE/SEI 41*, Reston, Virginia.

Bertero, V. and Brokken, S. (1983), “Infills in seismic resistant building”, *J. Struct. Eng. (ASCE)*, **109**(6), 1337-1361.

Buonopane, S.G. and White, R.N. (1999), “Pseudo-dynamic testing of masonry infilled reinforced concrete frame”, *J. Struct. Eng. (ASCE)*, **125**(6), 578-589.

Crisafulli, F.J., Carr, A.J. and Park, R. (2000), “Analytical modelling of infilled frame structures – A general review”, *Bull. New Zealand Soc. Earthq. Eng.*, **33**(1).

Comite Europeen de Normalisation, “European standard EN 1998-3 Eurocode 8: design of structures for earthquake resistance – Part1: general rules, seismic actions and rules for buildings,” Brussels, 2004.

Fardis, M.N. and Panagiotakos, T.B. (1997), “Seismic design and response of bare and masonry-infilled reinforced concrete buildings, Part II: Infilled structures”, *J. Earthq. Eng.*, **1**(3), 475-503.

Fiore, A., Netti, A. and Monaco, P. (2012), “The influence of masonry infill on the seismic behaviour of RC frame buildings”, *Eng. Struct.*, **42**, 133-145.

Karsan, I.D. and Jirsa, J.O. (1969), “Behaviour of concrete under compressive loading”, *J. Struct. Div. (ASCE)*, **95**, ST 12, 2543-2563.

Kent, D. C., and Park R. (1971), “Flexural members with confined concrete”, *J. Struct. Div. (ASCE)*, **97**, ST 7, 1969-1990.

Klingner, R.E. and Bertero, V.V. (1978), “Earthquake resistance of infilled frames”, *J. Struct. Div. (ASCE)*, **104**(6), 973-989.

Lee, H.S. and Woo, S.W. (2002), “Effect of masonry infills on seismic performance of a 3-storey RC frame with non-seismic detailing”, *Earthq. Eng. Struct. Dyn. (EESD)*, **31**(2), 353-378.

Madan, A., Reinhorn, A.M., Mander, J.B. and Valles, R.E. (1997), “Modelling of masonry infill panels for structural analysis”, *J. Struct. Eng. (ASCE)*, **123**(10), 1295-1302.

Magenes, G. and Pampanin, S. (2004), “Seismic response of gravity-load designed frames with masonry infills”, *The 13th World Conference on Earthquake Engineering* , Vancouver, Canada.

Mahin, S.A. and Shing, P.B. (1985), “Pseudo-dynamic method for seismic testing”, *J. Struct. Eng. (ASCE)*, **111**(7), 1482-1503.

Mehrabi, A.B., Shing, P.B., Schuller, M.P. and Noland, J.L. (1996), “Experimental evaluation of masonry-infilled RC frames”, *J. Struct. Eng. (ASCE)*, **122**(3), 228-237.

Mosalam, K.M.A., White, R.N. and Ayala, G. (1998), “Response of infilled frames using pseudo-dynamic experimentation”, *Earthq. Eng. Struct. Dyn.*, **27**(6), 589-608.

Polyakov, S.V., “On the interaction between masonry filler walls and enclosing frame when loaded in the plane of the wall,” Earthquake Engineering, EERI: 1960, San Francisco, 36-42.

Pujol, S. and Fich, D. (1979), “The test of a full-scale three-story RC structure with masonry infill walls”, *Eng. Struct.*, 32(10), 3112-3121.

Stafford Smith, B. (1966), “Behaviour of square infilled frames”, *J. Struct. Div. (ASCE)*, **92**(1), 381-403.

Stafford Smith, B. and Carter, C. (1969), “A method of analysis for infilled frames”, *Inst. Civil Eng.*, **44**.

Stafford Smith, B. (1967), “Methods of predicting the lateral stiffness and strength of Multi-storey infilled

frames", *Build. Sci.*, **2**, 247-257.
Uva, G., Raffaele, D., Porco, F. and Fiore, A. (2012), "On the role of equivalent strut models in the seismic assessment of infilled RC buildings", *Eng. Struct.*, **42**, 83-94.

SA